Control and Cybernetics

vol. **40** (2011) No. 2

Detecting epileptogenesis in power variant domains*

by

Rory A. Lewis[1,2], Brian Parks[2], Doron Shmueli[1] and Sara Capinst[1]

[1]Departments of Pediatrics & Neurology, University of Colorado Denver
Anschutz Medical Campus, Colorado 80045, USA

[2]Department of Computer Science, University of Colorado at Colorado Springs
Colorado Springs 80918, USA

Abstract: This paper presents the merging of two sets of experiments in the continuing endeavor to mine epileptiform activity from Electroencephalograms (EEG). The goal is to develop robust classification rules for identifying epileptiform activity in the human brain. We present advancements using the author's proprietary developed spectral analysis software to link power spectra of rat EEGs experiencing epilepsy seizures with the authors DFA algorithm and their MATLAB spectral analysis. Our system links 1) power spectra of seizures, in sleep, spike and seizure states, with 2) Deterministic Finite Automata (DFA). Combining power spectra with DFA to correctly predict and identify epileptiform activity (spikes) and epileptic seizures opens the door to creating classifiers for seizures. We also present a DFA that separates the states between seizure and non-seizure using robust testing and additional algorithms to increase the rigor when the methodology analyses noisy signals. Our results show optimal identification of seizures even when significant artifact and noise is present in the polyphonic domain. Herein we present a dual methodology that increases epileptoid identification in a noisy domain that links time and frequency domain components from MATLAB and proprietary software to clinical epileptiform activity.

Keywords: intracortical electroencephalograms, discrete finite automata, epilepsy, Fourier transforms, rough sets.

1. Introduction

Probing human brain dynamics is complex yet necessary for predicting transient events which may occur before epileptic seizures. Unfortunately, 30% of patients that suffer from epilepsy are not well controlled on medication. Only a small fraction of these can be helped by seizure surgery, Firpi et al. (2005). Therefore, it would be life changing to a large number of individuals if a system

*Submitted: September 2010; Accepted: June 2011.

could be developed that would predict a seizure hours, minutes, or even seconds before its clinical onset because then strategies such as automated medication from implant devices, Eder et al. (1997); Stein et al. (2000), electrical stimulation, Schiff et al. (1994); Velasco et al. (2005), or local cooling, Gluckman et al. (2006), could be utilized to offset a clinical onset, Mormann et al. (2003). Recent research suggests that epileptic seizures begin as electrophysiological events starting up to 7 hours before a clinical onset, Litt et al. (2001). Even though these epilepsy patients only spend a small percentage of their lives actually having a seizure, it is common to hear that the real pain occurs during the interictal interval, when not having seizure, because the fear of the next seizure and the feeling of helplessness associated with it destroys their life, Fisher (1935)[????]. The challenge is that the dimensionality is huge; in the human brain there are approximately 100 billion neurons, each with about 1000 connections (synapses) Williams and Herrup (1988). Even in the rat brain it is estimated that there are approximately 200 million neurons, Korbo (1990); Bandeira et al. (2009). The connections are wired such that the problem is highly nonlinear. In a certain class of seizures it would be helpful if they could be detected even a few seconds prior to the start of a seizure. The dimensionality of the problem can be significantly reduced, with only a minimal loss of information by recording electrical potentials at multiple points on the surface of the skull or, using depth electrodes, in the hippocampus (EEG). Electroencephalograms (EEG) are accepted as one of the best means of evaluating neurocognitive functions, Niedermeyer and da Silva (1999). Seizure prediction is made more complicated in that a single individual's seizures are not alike, seizures from different individuals vary significantly, there is no single metric that consistently changes during all seizures and correlation among channels can change significantly from one seizure to the next, and even experts disagree as to what constitutes a seizure, Williams et al. (2007). For the reasons listed above, rigid seizure detection rules do not produce good results, Hellier et al. (2009), Williams et al. (2009). Interictal spikes are brief (20 - 70 ms) sharp spikes of electrical phenomena that stand out when compared to background EEG rhythms and may be indicative of an underlying epileptic process. Because they are considered as an indicator of the presence of epileptic seizures, and may actually precede a seizure (sentinel spike), the detection of these interictal, transient spikes which may be confused with artifact or noise is indeed a crucial element in the prediction of epileptic conditions.

Until 1992 most EEG analysis was based on analysis of brain slices, Molnar and Nadler (1999), or anesthetized animals, Buckmaster and Dudek (1998). Kainic acid, a chemoconvulsant extracted from seaweed, was introduced to induce seizures in animals. This provided a major breakthrough, particularly with the advent of monitoring the animals on video, but the equally significant subclinical seizures were impossible to detect with video monitoring alone. The field was further advanced through the development of a tethered recording system, Bertram et al. (1997), in which multi-channel cortical and sub-cortical record-

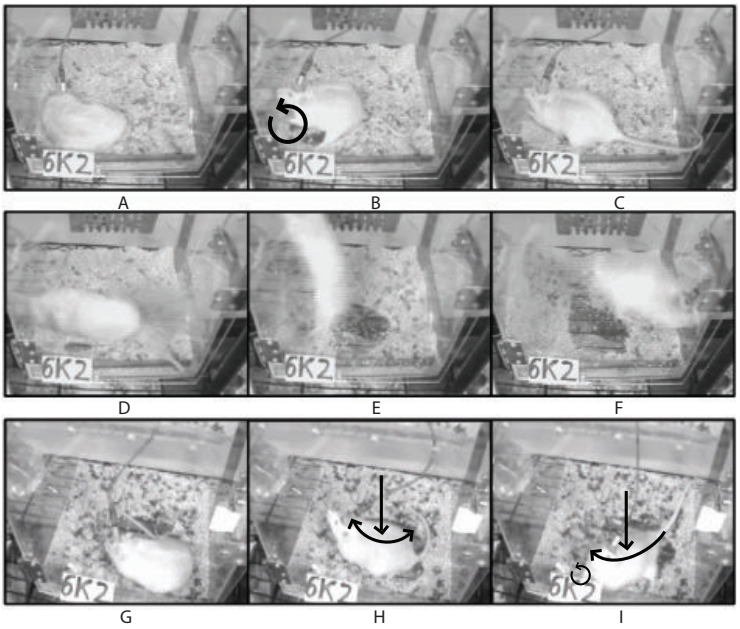

Figure 1. Video capture Rat 6K2: Progression of a Clinical convulsive seizure: **Series 1 (A-F):** (A) Rat in a normal sleeping stage. (B-C) Rat exits sleeping stage and starts having a P3 seizure (racine scale). (D-F) Seizure magnitude escalades to a violent uncontrollable seizure - P5 (racine scale). **Series 2 (G-I):** (G) Seizure detected before rat is aware of it. (H) Rat starts feeling clinical onset of seizure and arches its back. (I) P2 seizure with fully arched back and tail, jaw gnashing and one forelimb clonus

ings could be obtained. The quality of recordings were further improved by incorporating a small pre-amplifier close to the skull, allowing for a significant increase in the signal to noise (S/N) ratio. As shown in Fig. 1, electrodes were placed stereotaxically in the hippocampus and secured in the skull, Williams et al. (2006), White et al. (2006). Additional electrodes were placed directly on the dura. Dental cement was applied to hold the electrode pins together in a plastic cap that was later connected to the pre-amplifier. The pre-amplified signal was sent to an amplifier and from there to a computer for storage. This paper improves upon the methods set forth in the authors' previous work in Lewis et al. (2010) and Lewis and White (2010) by optimizing the DFA to efficiently recognize artifact and noise or analyzing the EEG of a rats experiencing P1 to P5 Seizures, Racine (1972). As seen in Fig. 1:

Series 1, Frames A-F Rat experienced a kainite-induced seizure that evolved from stage P3 to P5. In Frame A, the rat was sleeping. In Frame B, 58 seconds later, the rat experienced a P3 seizure evidenced by the circular

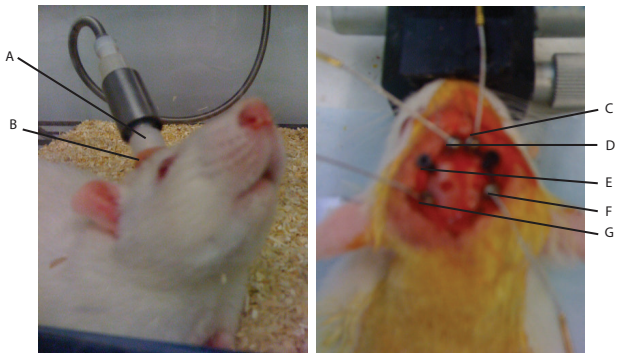

(a) (b)

Figure 2. Implantable Tethered System Devices: (A) Tethered pre-amplifier connects to the implanted electrodes and sends the signals to Epilepsy Monitoring Unit. (B) Dental cement polymer holds the electrodes in place. (C,D,F) Referential and positive leads for the dural EEG. (E) Stereotaxic placement of cortical electrodes. (G) Ground lead

clawing (forelimb clonus). In Frame C, 28 seconds later, convulsive activity stopped and there was no epileptic activity on the EEG. Frame D was taken 1 minute later and at this point the rat began to experience a P5 seizure that lasted several seconds. Frames E and F were taken subsequently and demonstrate the intensity of the seizure. Not seen in this figure is that this rat was eating calmly shortly after the end of the seizure.

Series 2, Frames G-I Unbeknownst to rat, while still sleeping in Frame G, it begins to experience a kainite-induced seizure. 27 seconds later in Frame H the rat begins to feel the clinical onset of the seizure we detected earlier. In Frame I it has developed to full P3 seizure with fully arched back, extended tail, jaw gnashing and forelimb clonus.

Our facility has the capability of continuously monitoring up to 64 tethered or untethered rats. Untethered rats underwent video monitoring and the tethered rats underwent both video and EEG monitoring. This paper will discuss the author's algorithms and power spectra methodology for analyzing the EEGs of two rats in experiencing three separate sequences of events wherein each sequence is divided into 3 states: (1) Sleep – Asleep, 60 seconds prior to a seizure, (2) Spike – Coincident with the Sentinel spike and (3) Seizure – Activity during clinical onset. As seen in Figs. 7, 8 and 9, two rats experience the aforementioned states that provide a controlled environment to perform the analysis necessary to compute the power spectra evoked by rats at critical points in each of the aforementioned "states". Furthermore, the authors have used the same environment to successfully 1) predict epileptiform activity using DFA (see Lewis et al., 2010) and 2) use their Integrated Power Spectral Difference

(IPSD) to detect the relationship that exists between channels once rats enter into a state of seizure, Lewis and White (2010). The availability of EEG data for this seizure and two other similar seizures, along with video, allowed us to test the hypothesis that a novel deterministic finite automata (DFA) methodology will be able to differentiate the different aspects (sleeping, P3 seizure, between seizures, and P5 seizure) of the EEG record. Working with the knowledge of the IPSD, and the DFA that provide EEG relationship, where prediction is known, we now present a means to correlate power spectra to known environments that will enable classification rule extrapolation.

2. EEG analysis & method

For our analysis EEG potentials were sampled at 800Hz. EEG electrodes were placed bilaterally in the hippocampi (referenced to a common dural screw) and a separate channel recorded from the dura. Each EEG contains approximately 100,000 time points. As such, its interpretation is non-trivial, and attempts at automating the analysis have met with only limited success. In this paper, we seek to demonstrate the efficacy of the DFA algorithm to distinguish all three states in each seizure event and distinguish artifact from interictal spikes and other noise. The author has begun to integrate statistical analysis with Action Rules (Lewis and Raś, 2007; Raś and Dardzińska, 2005; Raś and Wieczorkowska, 2000; as well as Pawlak, 1991; Raś et al., 2005; Tsay and Raś, 2005). We are also experimenting with Fourier Action Rules Trees of signal distortion, Lewis and Wieczorkowska (2007), and Machine Learning with Signal Noise, Genetic algorithms, Lewis et al. (2008), FS-trees, Rough Sets, LERS & Orange, Lewis et al. (2007).

Fig. 3§1 illustrates one rat's normal EEG wave-form while asleep. Point II in Fig. 3§1 illustrates a Sentinel Spike, the hallmark indicator that a seizure is imminent. Point III in Fig. 3§1 shows a region in which the EEG record deviates from baseline. An important task is to determine whether this deviation is simply an artifact or if it represents epileptiform activity (an interictal spike). Fig. 3§2 provides details of the P3 seizure. Fig. 3§3 provides a zoomed-out overall view of all four stages and Fig. 3§4 provides details of the P5 (Racine scale) stage. We utilized two sets of experiments, both of which use EEG potentials sampled at 800Hz, where the electrodes were placed bilaterally in the hippocampi (referenced to a common dural screw) and a separate channel recorded from the dura. The first experiment use DFA to test when the system state would change dependent on such quantities as amplitude, slope, second derivative, Short-Term Fourier Transform. In the second experiment we compare the aforementioned states, given the results in experiments, while comparing distances of sleep and seizure in our sample domain. The authors used DFA in Lewis et al. (2010) and Lewis and White (2010) using the European Data Format (EDF) to track the current state of a finite-state EEG system. As time moved forward, the particular system state changed amplitude, slope,

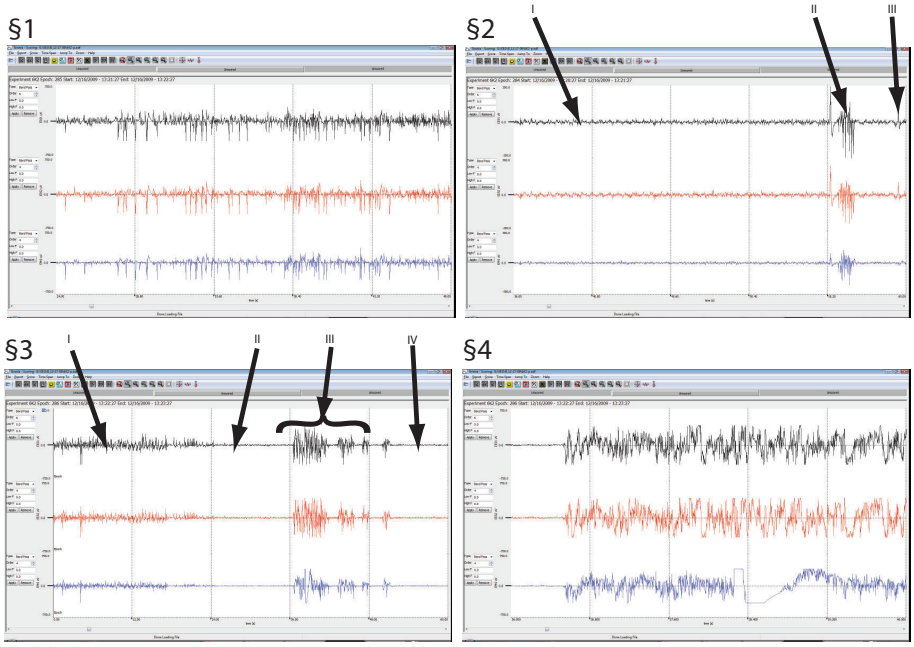

Figure 3. Rat P3 seizure (Racine scale): **§1:** 6K2 EEG state correlating to Fig. 1 Stage B denoted by circular clawing **§2:** I. Normal EEG wave-form while Rat is a sleep. II. Appearance of Sentinel Spike prior to P3 (Racine scale) seizure. III. Possible Interictal Spike often misinterpreted as artifact and vice-versa. **§3:** I. A P3 (Racine scale) seizure in progress. II. Period of no Electrographic seizing activity. III. Electrographic outburst indicating the violent seizure time. IV. End of Electroencephalographic seizure event. **§4:** Covers periods D, E and F in Fig. 1 showing the EEG analysis while 6K2 experiences the P5 (Racine scale) seizure.

second derivative, Short-Term Fourier Transform STFT (average frequency) as well as other signal features. At time zero we begin at state zero. The state at the next time step is assumed to be dependent only on the current system state and conditions (input state) during the current time step (e.g. slope). A consequence of this is that the current state is independent of the order, in which the input states occurred (in this sense it is similar to a Markov chain).

3. Illustrative example of our DFA methodology

To motivate reader understanding we illustrate the concept of our usage of DFA using a simplified transition table given in Fig. 4, composed of ten columns. The first column is the current system state. As one moves from one time point

of the EEG to the next, the state of the system changes. The state to which the system changes is based upon the transition matrix; each of the columns in the transition matrix represents a current parametric set (e.g. slope within a particular range). More generally, the columns may represent a condition in which current or past parameters have specified values. It should comprise a collectively exhaustive and mutually exclusive set such that there are no events that either fall into multiple columns or do not fall into any of the columns. One proceeds from one system state at a given time point to the next system state at the next time point until a terminal event occurs. Terminal events can be the identification of spikes, seizures or artifact. The particular input state at the current time (columns 5 - 10) is ascertained by investigating parameters at that time or at prior times. For this example, we have six mutually exclusive, collectively exhaustive input states. These are presented in Table 1 where α, β, and γ are limits selected by the authors using expert knowledge of what parameters would be characteristic of spikes. We note that states 4, 5 and 6 are the same as 1, 2, and 3, except that the absolute value of the second derivative ($f"(x)$ or $\frac{d^2y}{dt^2}$) is less than γ. The purpose of the use of slope ($m = \frac{y_2-y_1}{t_2-t_1}$) is to differentiate between the normal state, the possibility of a spike, and a likely artifact (artifact, such as that noted when the animal is chewing, is often distinguished from spike because the slope is much greater).

State	# of 1/4	# of 2/5	# of 3/6	Input 1	Input 2	Input 3	Input 4	Input 5	Input 6
0	0	0	0	0	2	0	0	2	0
1	0	0	1	0	3	0	0	3	0
2	0	1	0	10	4	3	10	4	3
3	0	1	1	11	5	0	11	5	0
4	0	2	0	12	6	5	12	6	5
5	0	2	1	13	7	0	13	7	0
6	0	3	0	14	6	7	14	16	7
7	0	3	1	15	7	0	15	16	0
8	1	0	0	0	10	0	0	10	0
9	1	0	1	0	11	0	0	11	0
10	1	1	0	0	12	11	0	12	11
11	1	1	1	0	13	0	0	13	0
12	1	2	0	0	14	13	0	14	13
13	1	2	1	0	15	0	0	15	0
14	1	3	0	0	14	15	0	16	15
15	1	3	1	0	15	0	0	16	0
16	0	0	0	24	18	17	24	18	17
17	0	0	1	25	19	0	25	19	0
18	0	1	0	26	20	19	26	20	19
19	0	1	1	27	21	0	27	21	0
20	0	2	0	28	22	21	28	22	21
21	0	2	1	29	23	0	29	23	0
22	0	3	0	30	22	23	30	32	23
23	0	3	1	31	23	0	31	32	0
					⋮				
n-1	1	3	0	0	30	31	0	32	31
n	1	3	1	0	31	0	0	32	0

Figure 4. Sample Transition Table: the number of possible states is 31, the number of states with slope too high required for rejection is 2, number of states required for slopes in the range for acceptance is 4, and the number of states with slope too low requiring rejection is 2

Table 1. Six mutually exclusive, collectively exhaustive input states. Where α, β, and γ are user selected constants. States 4, 5 and 6 are the same as 1, 2, and 3 except that the second derivative is less then a given value

	Input State Conditions
1	$\mid m = \frac{y_2 - y_1}{t_2 - t_1} \mid > \alpha \wedge \mid f"(x) or \frac{d^2y}{dt^2} \mid < \gamma$
2	$\alpha > \mid m = \frac{y_2 - y_1}{t_2 - t_1} \mid > \beta \wedge \mid f"(x) or \frac{d^2y}{dt^2} \mid < \gamma$
3	$\mid m = \frac{y_2 - y_1}{t_2 - t_1} \mid < \beta \wedge \mid f"(x) or \frac{d^2y}{dt^2} \mid < \gamma$
4	$\mid m = \frac{y_2 - y_1}{t_2 - t_1} \mid > \alpha \wedge \mid f"(x) or \frac{d^2y}{dt^2} \mid > \gamma$
5	$\alpha > \mid m = \frac{y_2 - y_1}{t_2 - t_1} \mid > \beta \wedge \mid f"(x) or \frac{d^2y}{dt^2} \mid > \gamma$
6	$\mid m = \frac{y_2 - y_1}{t_2 - t_1} \mid < \beta \wedge \mid f"(x) or \frac{d^2y}{dt^2} \mid > \gamma$

The purpose of the use of $f"(x)$ is to ensure that there is actually a peak and not just a baseline shift. Columns 2 - 4 indicate the number of times that input states 1 or 4, 2 or 5, or 3 or 6, respectively, have occurred. For example, looking at system state 12 one notes that there has been a single event in which the input state 1 or 4 existed, two events in which input state 2 or 5 existed and no events in which the state 3 or 6 existed. To register a spike, there must be two time points in which ($m = \frac{y_2 - y_1}{t_2 - t_1}$) falls in the range expected for a spike (input states 2 or 5), followed by one time point in which $f"(x)$ is high (input state 5) which corresponds to a peak, followed by two time points in which the slope again falls in the correct range (input states 2 or 5). This sequence must occur before one obtains two slopes greater than the range or two slopes less than the range. In this example a spike is indicated by system state 32. A heuristic definition can then be used to establish the seizure state by requiring a certain number of spikes in a particular time interval (e.g. 20 detected spikes in 10 seconds).

We now consider the sample path through the transition matrix illustrated by the chain of circles noted. For this sample the sequence of input states is assumed to be: $2, 2, 3, 1, 2, 5, 5, 5, 5$. We initially start with state 0, time interval 0. At this time, the slope was calculated to be appropriate for a spike, i.e. $\alpha <\mid slope \mid < \beta$, with the second derivative $< \gamma$ (input state = 2). As a result the transition matrix indicated a change to system state 2. For the second time interval the input state was calculated to be the same as that in the first time interval (input state = 2), and the transition matrix (row 3, column 6) indicated a change to system state 4. In the next time interval input state 3 was calculated

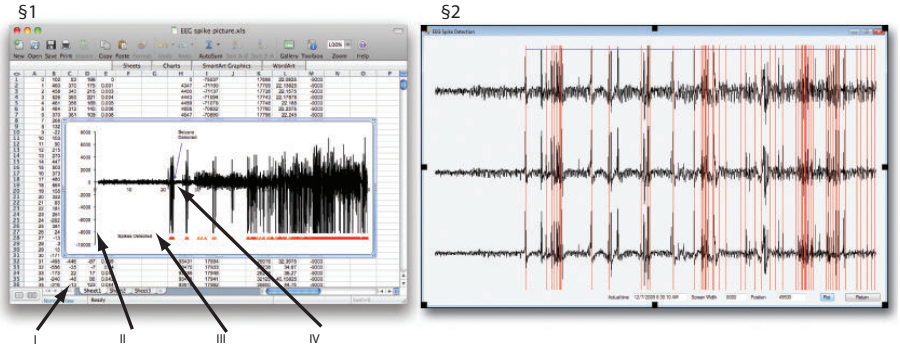

Figure 5. Results: Seizure Correctly Predicted I: **§1:** Code correctly identifies a seizure 6 seconds before its onset. **I.** Excel Spreadsheet with CSV output. **II.** Excel built in graph. **III.** The "Spikes Detected" references and ***IV.*** Seizure Detected at location 6 seconds before onset. **§2:** Initial portion of seizure. Notice both high frequency, low amplitude spikes as well as higher-amplitude, lower frequency spikes. The vertical lines in the figure indicate spikes detected using the DFA algorithm. The lighter shaded line in the figure indicates the detected start of seizure as determined by the heuristic requirement of 3 spikes per second for 10 seconds

and the system state of 5 (*row*5, *column*7) was determined. Subsequent input states could then be coupled with the current system states to draw a time path through the transition matrix. In this case, a spike is registered at the end of the path because state 32 is obtained at the end of the chain. Had there been too many slopes that did not meet criteria, the system state would return to zero (see for example system state 9, input state 1).

3.1. Experiment 1: Seizure prediction using DFA

Using the same six input states given in the example above to determine the input state we used only the slope and standard deviation. In the first seizure (*Series 1*, Frames A-F, see Fig. 1) the system is able to successfully differentiate between true interrictal spikes, which often precede the onset of seizure, and artifactual spikes, which appear similar to interrictal spikes to the untrained eye, but do not immediately precede seizure. Fig. 5 demonstrates the former, showing the interrictal spike preceding the seizure depicted in Fig. 1 by 6 seconds. In the second seizure, (*Series 2*, Frames G-I, see Fig. 1) the system first detected the 2nd seizure while the rat was asleep and oblivious to the oncoming seizure (see Frame G, Fig. 1) The authors note that the interictal spike shown at this point, 57 seconds before the seizure begins, was too abrupt for the DFA to classify it as a seizure spike. However, a few seconds later as we get to signals

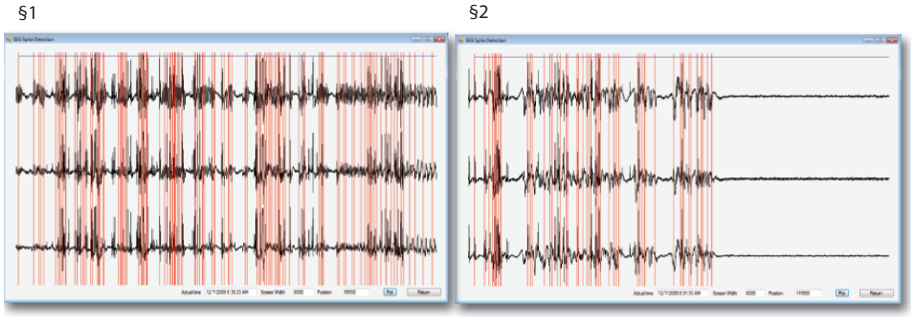

Figure 6. Results: Seizure Correctly Predicted II: **§1:** Continued seizure activity indicated by high frequency medium amplitude discharges. **§2:** Seizure end. Note the abrupt discontinuation of EEG seizure discharge. The seizure duration is approximately 90 seconds

exemplified in Fig. 5§2. The seizure does indeed begin. The authors added a screen output of steep vertical lines where the methodology detected a spike using the DFA algorithm. Note that we also added a line in the figure that indicates the detected start of seizure as determined by the heuristic requirement of 3 spikes per second for 10 seconds. This state occurs 13 seconds after the detected interictal spike warns the DFA that a clinical onset is beginning. In essence, Figs. 5 and 6 show various segments of EEG data from rat 6K2 seizure. Fig. 5§1 shows the onset of the *Series 1* seizure looking at the raw CSV file, demonstrating the characteristics used in this study. Here the output is a successful detection within 6 seconds of clinical onset. Similarly, Fig. 5§2 shows the onset of the *Series 2* seizure where each of the steep vertical lines denotes a spike detected using the DFA technique described herein indicating the duration of the seizure. The range was determined by spike frequency using a heuristic approach of 3 or more spikes per second over each of 10 consecutive seconds. Fig. 6 shows the continuation of this characteristic EEG activity over the 90-second duration of the seizure, which ends with the activity shown in Fig. 6. Furthermore, Fig. 6 shows continued DFA detection of the *Series 2* seizure where the steep vertical lines exemplify an intense seizure where the rat arches its back in (see Fig. 1 images H and I). More significant, however, is that the DFA detected this when the seizure was in its infancy.

3.2. Experiment 2: EEG analysis

Our experiment methods comprised three sections. First using MATLAB to extract and plot critical sequences, secondly performing an FFT using a rectangular or Dirichlet window using Visual Studio and thirdly, using DFA to track the current states of amplitude, slope, second derivative and Short-Term

Fourier Transform STFT. For a particular time interval we perform an FFT using a rectangular or Dirichlet window (optionally Hamming or Hann windows may also be used to reduce abrupt window cut off effects) to establish the real and imaginary parts in the frequency domain, i.e.

$$Re\,(f) = \sum_{k=1}^{n-1} x_k \cos 2\pi \left(\frac{kp}{n}\right) \tag{1}$$

$$Im\,(f) = \sum_{k=1}^{n-1} x_k \sin 2\pi \left(\frac{kp}{n}\right). \tag{2}$$

We then compute the power in each frequency bin, whose width is $\Delta f = \frac{sampling\ frequency}{time\ interval\ width}$, (where the sampling frequency is measured in points per second and the interval width is measured in points per time interval) as $Re\,(f)^2 + Im\,(f)^2$. The time interval in the study has been chosen to be long enough to capture several individual spike components, but short enough so that an early detection is feasible. Our current time interval is set at 0.64 seconds (512 points at 800 points/second). Lower and upper frequency bounds are created that reflect frequencies we expect to find during a seizure (currently between 3 and 50 Hz). The authors introduce a metric defined as the Integrated Power Spectral Difference (IPSD) whereby we compare the power spectra in either (1) a single channel at two successive time intervals, or (2) two separate channels at the same time interval. The motivation for this was that there is a need to see how close one frequency distribution is to the next, because we suspect that during a seizure successive frequency distributions and powers spectra will be similar in any particular channel between one time point and the next. Mathematically, we define this metric as:

$$IPS(f) = \int_{freq\ low}^{freq\ high} PS(f)df. \tag{3}$$

This is akin to comparing cumulative distribution functions rather than probability density functions. We use this metric rather than just subtracting the power spectra at each individual frequency to allow us to capitalize on the evolution of seizures. As seizures evolve, the frequency tends to slow and the amplitude increases. The formulation used here penalizes this frequency shift less than that which would occur if the power spectra were directly subtracted. Because seizures are not strictly focal phenomena, and often impact distant regions, one would expect significant correlation among the different channels.

$$IPS = \int_{freq\ low}^{freq\ high} \Big| IPS_{T_1}(f) - IPS_{T_2}(f) \Big| df \tag{4}$$

where $PS(f) = Power\ Spectrum$ of channels 1 and 2 respectively when two

successive time intervals for a single channel are considered, and as

$$IPS = \int_{freq\ low}^{freq\ high} \Big| IPS_{ch_1}(f) - IPS_{ch_2}(f) \Big| df \tag{5}$$

when two different channels are considered at the same time interval. We note that these metrics are in no sense unique. We have employed other metrics such as difference in median, mean and modal frequencies, as well as using frequency weighting (adding more weight to differences in higher frequencies). Upon comparing these metrics, it appears that integral method more accurately separates seizure from non-seizure states.

4. Deterministic Finite Automata (DFA)

Deterministic finite automata can be used in many applications. We used this methodology to track the current state of a finite-state EEG system. As time moved forward, the particular system state would change dependent on such quantities as amplitude, slope, second derivative, Short-Term Fourier Transform STFT (average frequency) as well as other signal features. For the current analysis, programming was done using Visual Basic subroutines and data was stored using the European Data Format (EDF). At time zero we begin at state zero. The state at the next time step is assumed to be dependent only on the current system state and conditions (input state) during the current time step (e.g. slope). A consequence of this is that the current state is independent of the order in which the input states occurred. Experiments consisted of comparing two spectral analysis methodologies that honed in on a first 60 second period before clinical onset, which in these cases was purposefully chosen to be a sleep state and then next the spike, interictal and seizure states of the animal. Upon using Matlab EEGLAB package, analyzing the signals and then normalizing the sleep to zero and then performing the numerical normalization we performed on the sleep to the spike and seizure states we found an interesting pattern suggesting rules as seen in Fig. 13. We decided to then code our own, more in-depth spectral analysis using Visual Studio that was able to detect parameters in a way easier than that found in Matlab. It is critical to note that our DFA has already located these sections of EEG to be that of a seizure state. After opening an EDF file in EEGLAB (using the Import Data > From EDF Files menu option) the raw data is available in the "data" attribute of the "EEG" object. Plotting a particular row of this variable using the Matlab "plot" command (e.g.: "plot(EEG.data(2,:))") shows the raw data for the respective channel, from which it is fairly trivial to determine the range of samples corresponding to a particular feature of the EEG signal. Using the x values shown on this plot and dividing by the sample rate (in our case, 800 Hz), we can obtain the number of seconds into the recording that the feature occurred, entering it into the dialog presented by the Plot > Channel Spectra and Maps menu

option (after multiplying by 1000 to convert to milliseconds). Since our features corresponded to .64 seconds (starting at n milliseconds as determined above), we specified the range to be "n, $n+640$" and encompassing 100 % of the signal in that range.

5. Spectral analysis method: in-house Visual Studio implementation

5.1. Spectral data

This consisted of two code sections. The first of these was concerned with establishing the power spectra for the three-channel EEG data. The second implemented the DFA algorithm to identify seizures. For the first section, we used sequential Fast Fourier Transforms on 2.5 second (2048 point) intervals of EEG data. The spectra were derived using rectangular windows with a low frequency bound of 3 Hz and a high frequency bound of 70 Hz. Spectral plots were created using 40 successive time intervals with no overlap, as shown in Fig. 14. The IPSD metric was calculated at every time interval. The DFA portion of the code used the IPSD metric and a transition table to identify seizure events. There were three possible input states for the matrix: (1) IPSD $> a$, (2) IPSD $< a$, but $> b$, and (3) IPSD $< b$, where a and b are constants that were empirically derived. This operation was performed comparing all times with successive times and all combinations of channels. The number of transition matrix states was 36. A seizure was identified if greater than a specified number of input state (2) occurred prior to a given number of state (1) or (3) occurring. Performing the power spectra and with the correlated DFA on the 3 sequences comprising each of the 3 states as seen in Figs. 7, 8 and 9 we see resultant 4 states of the power spectra provided in Fig. 10 showing the sleep power spectra, Fig. 11 showing the spike power spectra and Fig. 12 showing the seizure power spectra. Here we will see three traces representing the EEG signals originating from the three electrodes placed in the animal's hippcami as illustrated in Fig. 1. Fig. 10 shows three sub-figures: sub-figure (a) illustrates the sleep power spectra of rat 8K1 in sub-figure (a) of Fig. 7, sub-figure (b) illustrates the sleep power spectra of rat 8K3 in sub-figure (a) of Fig. 8, and sub-figure (c) illustrates the sleep power spectra of rat 8K3 in sub-figure (a) of Fig. 9.

5.2. Spike power spectra

Fig. 11 shows three sub-figures: sub-figure (a) illustrates the spike power spectra of rat 8K1 in sub-figure (b) of Fig. 7, sub-figure (b) illustrates the spike power spectra of rat 8K3 in sub-figure (b) of Fig. 8, and sub-figure (c) illustrates the spike power spectra of rat 8K3 in sub-figure (b) of Fig. 9.

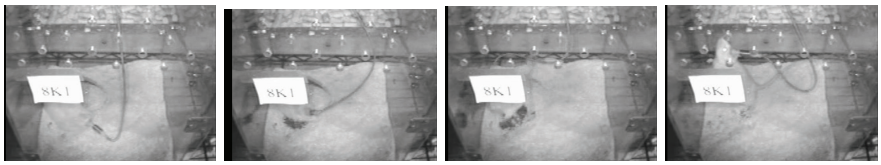

(a) (b) (c) (d)

Figure 7. A seizure detected in rat 8K1. (a) Rat is asleep prior to seizure. (b) Coincident with the sentinel spike, rat 8K1 wakes up. (c) Rat experiences seizure. (d) After seizure. Non-seizure rat activity

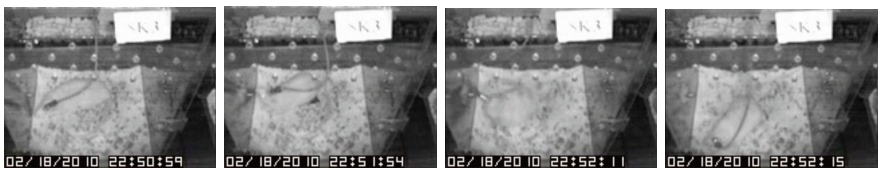

(a) (b) (c) (d)

Figure 8. A seizure detected in rat 8K1. (a) Rat is asleep prior to seizure. (b) Rat experiences sentinel spike and begins to engage in waking activity. (c, d) Peak seizure activity

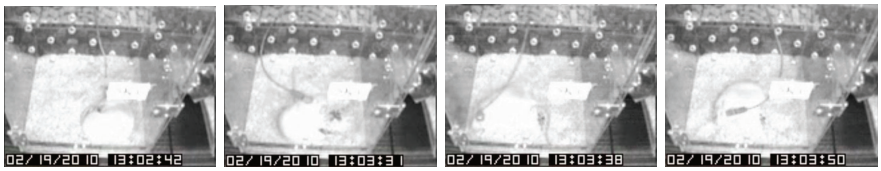

(a) (b) (c) (d)

Figure 9. A seizure in rat 8K3 occurring just over 14 hours subsequent to that depicted in 8. (a) Rat is curled up, asleep. (b) Peak seizure activity. (c) Seizure causes rat to fall across viewing area. (d) Rat seems dazed after seizure activity

5.3. Seizure power spectra

Fig. 12 shows three sub-figures: sub-figure (a) illustrates the seizure power spectra of rat 8K1 in sub-figure (d) of Fig. 7, sub-figure (b) illustrates the seizure power spectra of rat 8K3 in sub-figure (d) of Fig. 8, and sub-figure (c) illustrates the seizure power spectra of rat 8K3 in sub-figure (d) of Fig. 9. From the sleep power spectra it seemed that because our DFA predicted the seizure during the sleep states via the interictal spike, then the power spectra we are most likely concerned with are the properties of the interictal spikes and seizures incurred

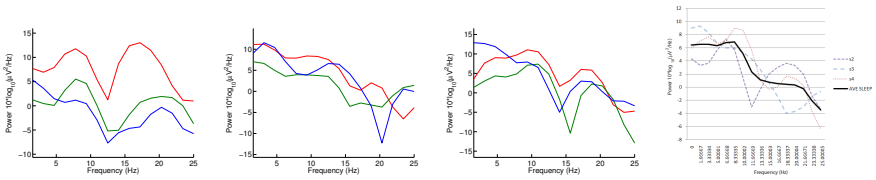

(a) (b) (c) (d)

Figure 10. Spectral Sleep States for seizures 2 (a), 3 (b), and 4 (c). Note there is an almost equal representation of lower frequency components and higher-frequency components, with consistent peaks at approximately 7 and 17 Hz. (d) illustrates the mean

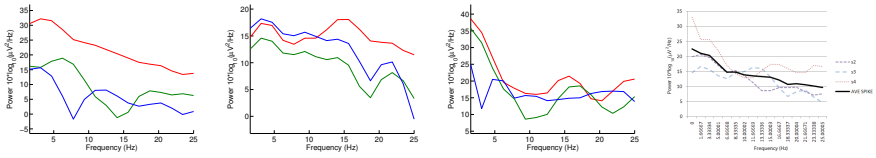

(a) (b) (c) (d)

Figure 11. Spectral Spike States. Note a marked increase in the amount of low-frequency EEG activity while the higher-frequency activity stays comparatively constant. (d) illustrates the mean

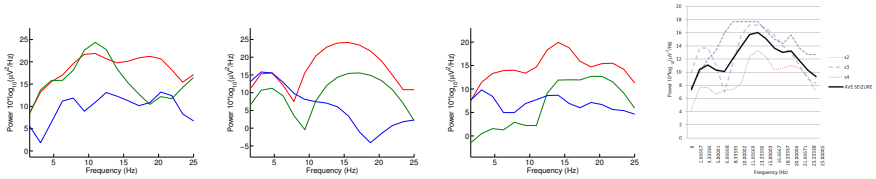

(a) (b) (c) (d)

Figure 12. Spectral Seizure. Note the prominent peaks in the higher-frequency portion of the plots representing the high-frequency neural discharge characteristic of seizure. (d) illustrates the mean

by the animal in relation to its sleep power spectra state. Fig. 13 shows a normalized power spectra of the sleep denoted by the dashed line at 0. The averaged line represents the mean on the Sleep state as shown in sub-figure (b) of Fig. 10 but in relation to its sleep state. Similarly, the power spectra of the seizure states as shown in sub-figure (d) of Fig. 10 are also depicted in relation to the animal's sleep state. The authors overlayed the linear progression of the the normalized spike and seizure states to illustrate where the power in

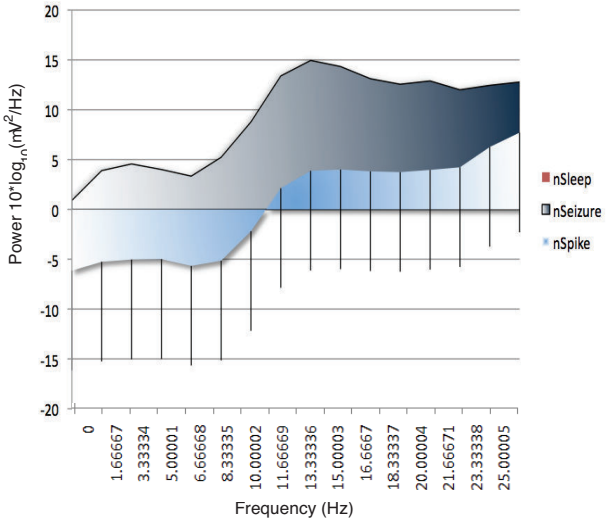

(a)

Figure 13. Normalized Sleep correlation to Spikes and Seizure.

the frequency domain is spread and focused during the interictal and seizure states in relation to the sleep state. We know that the DFA tells us that these states are correct in that they do represent the states leading to and during an epileptic seizure. Manipulating the power spectra in this form illustrates that certain characteristics of the power, when changing in accordance to the sleep state represent an interictal spike. For example, looking at Fig. 13, if a rat is asleep and the power frequency is normalized to zero across all bands, then if power at frequency 0 through to 8 Hertz is below zero and power of frequency 12 to 25 Hertz is in the range of 3 to 8 then the rat is probably experiencing an interictal spike. Similarly, if power at frequency 0 through to 8 Hertz is in the range of 3 to 8 and power at 12 - 25 Hertz is 8 to 15 then the rat is probably experiencing an seizure spike. The aforementioned results are illustrated in Figs. 14–17. Fig. 14 is a screenshot from OUR EEG-processing code showing EEG spectrogram. In Fig. 15 we see the spectral analysis of EEG signal during interictal period. The raw EEG is on the left side of the screenshot and on the right side one can see that the power spectrum at time t represents the same for time $t + \Delta t$. Note the significant difference in power spectra in each channel. The plot on the bottom left represents the background average spectra. Note that we constrain our analysis of the power spectrum from 3 to 70 Hz. In Fig. 16 we have displayed the Cumulative Distribution Function for the power spectra of EEG signal during non-seizure (interictal) state at time t and $t + \Delta t$. Note the significant difference between IPS (integrated power spectra) circled in the

plots on the right side of the figure. In Fig. 17 we see the IPSs for different time intervals for each channel on the right side of the figure. Note the IPSD metric will be significantly smaller here than in Fig. 16. This is a characteristic of the seizure (ictal) state.

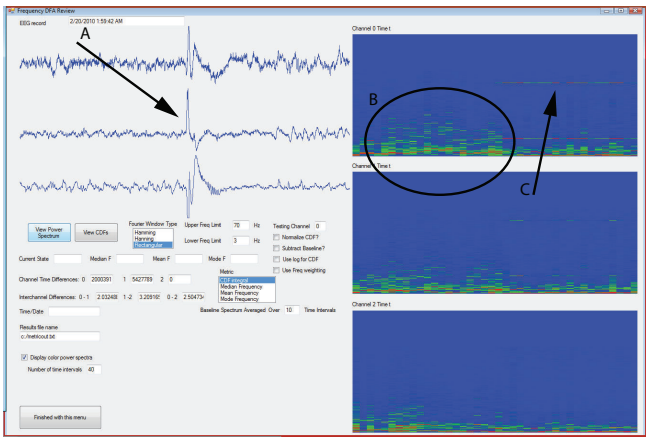

(a)

Figure 14. Screenshot from EEG-processing code of the EEG spectrogram. A,B,C. (A. Sentinel spike. B. Spectrogram of seizure. C. Generally the high-frequency noise present in the spectrogram after the seizure was found to be due to extraneous signal source).

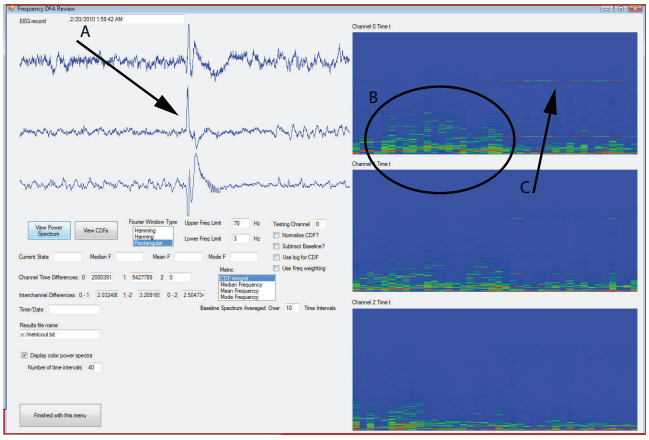

(a)

Figure 15. Spectral analysis of EEG signal during interictal period

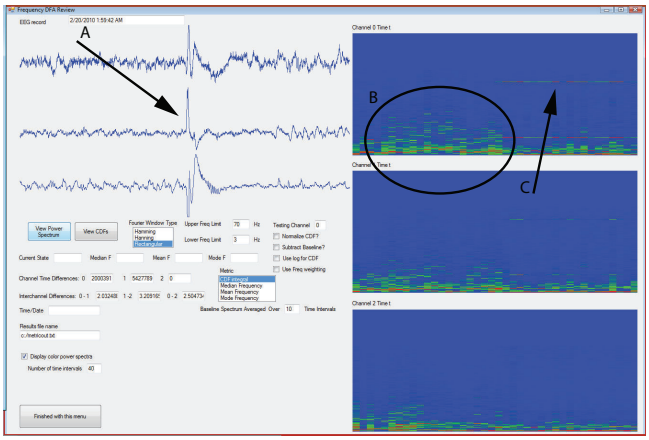

(a)

Figure 16. Cumulative Distribution Function for the power spectra of EEG

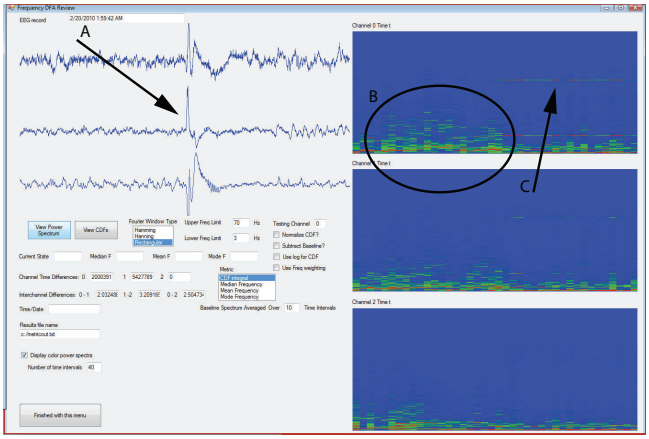

(a)

Figure 17. IPSs for different time intervals

6. Conclusion

Using our techniques described above, we performed calculations to determine seizure onset in a specific rat. It allowed us to identify seizure onset approximately 11 seconds after the sentinel spike. In this particular case, this was done using the IPSD metric between channels. The DFA allowed us to reject many other possibilities in this noisy signal. In Experiment 1 we found that in both Series 1 and 3 seizures the DFA correctly identified spikes and seizures sorting

various events that occur during seizures. This identification occurred in spite of a very noisy record. Given this noisy record, it is not possible for even an expert to determine with certainty that a particular event is a spike or seizure. It is certainly possible that a given EEG recording could result from either a spike or artifact (there is not necessarily a one-to-one and onto mapping). To the extent that it is possible, given enough input states, the algorithm is as capable as any expert to differentiate spike from non-spike or seizure from non-seizure states. Obviously, computational time limits the number of possible states, but this, as well as the particular parameters that characterize the input state, can be chosen to decrease the computational effort. It is not restricted to linear analysis such as Neural Networks, Random Forest and Machine Learning J45 to define strong classifiers for items such as Sentinel Spikes; it is also possible to use sequential non-linear analysis to establish whether or not spikes have occurred. By generalizing the input states to include past parameters, it is even possible to force the current state to be dependent on the path taken to get to the current state. The transition matrix can also be modified in such a way that multiple final deterministic states are possible (i.e. multiple end points could be identified). It is our plan to investigate further methods in which the DFA algorithm can be successfully employed. This includes the process of integrating KDD with the DFA methods and also considering the use of time domain analysis of EEG signal by statistical analysis and characteristics computation, Litt et al. (2001), with different frequencies, Salant et al. (1998), non-linear dynamics and chaos theory, Lehnertz and Elger (1995), and intelligent systems, such as artificial neural network and other artificial-intelligence structures, Geva and Kerem (1998), Pan et al. (2007). In Experiment 2, the authors introduced a new metric that is useful in establishing difference in power spectra between successive time intervals and different EEG channels. This metric uses the characteristic evolution of seizures to minimize differences from one time interval to the next one during a seizure event. We have shown that a combination of spectral analysis and DFA is a valid method for identifying seizure onset. It is anticipated that further improvement of the method can be achieved by investigating the characteristics of the change in the IPSD metric as a seizure progresses. This may be used in a training algorithm for an individual seizures. We have in essence narrowed the scope of the domain to a plausible state mathematically. Moreover the authors' Integrated Power Spectral Difference (IPSD) has double rechecked the range of EEG signals that are critical to perform Spectral Analysis on to Garner rules, see Lewis et al. (2010), Lewis and White (2010). Clearly, the broad rules set forth in this paper regarding spikes and seizures have not been proven to work over thousands of rats nor on humans to say the least. But we do know that with these three seizures, these power spectra rules certainly do work. For our future work we will have to first run exactly the same tests over many more rats and then test our hypothesis with Neural Networks, Random Forest and Machine Learning J45 to define strong classifiers.

Acknowledgment

This research was funded in part by the grant NINDS 5-K08 NS-053610-04.

References

Bandeira, F., Lent, R. and Herculano-Houzel, S. (2009) Changing numbers of neuronal and non-neuronal nells underlie postnatal brain growth in the rat. *Proceedings of The National Academy of Sciences of the USA* **106**(33), 14108–14113.

Bertram, E.H., Wiliamson, J.M., Cornett, J.F., Spradlin, S. and Chen, Z.F. (1997) Design and construction of a long-term continuous video-EEG monitoring unit for simultaneous recording of multiple small animals. *Brain Research Protocols* **2** (1), 85—97.

Buckmaster, P.S. and Dudek, F.E. (1998) Neuron loss, granule cell axon reorganization, and functional changes in the dentate gyrus of epileptic kainate-treated rats. *The Journal of Comparative Neurology* **385**(3), 385–404.

Eder, H.G., Jones, D.B. and Fisher, R.S. (1997) Diazepam prophylaxis for bicuculline-induced seizures: a rat dose-response model. *Epilepsia* **38**, 516.

Firpi, H., Goodman, E. and Echauz, J. (2005) Genetic Programming Artificial Features with Applications to Epileptic Seizure Prediction. *Engineering in Medicine and Biology Society, 2005. IEEE-EMBS 2005. 27th Annual International Conference, Shanghai*. IEEE, 4510–4513.

Fisher, R.A. (1935) The Logic of Inductive Inference. *J. R. Stat. Soc. A*, 98.

Geva, A.B. and Kerem, D.H. (1998) Forecasting generalized epileptic seizures from the EEG signal by wavelet analysis and dynamic unsupervised fuzzy clustering. *IEEE Transaction of Biomed Engineering*, **45**, 1205–1216.

Gluckman, B.J., Nguyen, H., Weinstein, S.L., Schiff, S.J. (2006) Adaptive electric field control of epileptic seizures. *The Journal of neuroscience: the official journal of the Society for Neuroscience*, **21**(2), 590–600.

Hellier, J., White, A.M., Williams, P.A., Dudek, E.F. and Staley, K.J. (2009) NMDA receptor-mediated long-term alterations in epileptiform activity in experimental chronic epilepsy. *Neuropharmacology* **56**(2), 414–421.

Korbo, L. (1990) An Efficient Method for Estimating the Total Number of Neurons in Rat Brain Cortex. *Journal of Neuroscience Methods*, **31**(2), 93–100.

Lehnertz, K. and Elger, C. (1995) Spatio-temporal dynamics of the primary epileptogenic area in temporal lobe epilepsy characterized by neuronal complexity loss. *Electroencephalography and Clinical Neurophysiology*, **95**, 108—117.

Lewis, R., Cohen, A., Wenxin, J. and Raś, Z.W. (2008) Hierarchical Tree for Dissemination of Polyphonic Noise. *Rough Sets and Current Trends in*

Computing. Proceedings of the 6th International Conference on RSCTC '08, Akron, OH. Springer-Verlag,Berlin-Heidelberg, 448–456.

Lewis, R. and Raś, Z.W. (2007) Rules for Processing and Manipulating Scalar Music Theory. *Proc. IEEE Computer Society April 26-28 MUE 2007 in Seoul Korea*, 819–824.

Lewis, R., Shmueli, D. and White, A.M. (2010) Deterministic Finite Automata in the Detection of EEG Spikes and Seizures. In: P.R. Cohen, N.M. Adams and M.R. Berthold, eds., *Advances in Intelligent Data Analysis IX.* **LNCS 6065**, Springer, 103–113.

Lewis, R. and White, A.M. (2010) Seizure Detection Using Sequential and Coincident Power Spectra with Deterministic Finite Automata. In: *Proceedings of Bioinformatics and Computational Biology (BIOCOMP) 2010*, Las Vegas Nevada, Volume II. World Academy of Science, 481–488.

Lewis, R. and Wieczorkowska, A. (2007) Categorization of Musical Instrument Sounds Based on Numerical Parameters. In: *Proceedings of RSEISP, 15th International Conference on Conceptual Structures, ICCS 2007, Sheffield, UK.* **LNAI 4604**, Springer Berlin-Heidelberg, 784–792.

Lewis, R., Zhang, X. and Raś, Z.W. (2007) MIRAI: Multi-hierarchical FS-Tree Based Music Information Retrieval System. **LNAI** [Volume no.??], Springer, 28–30.

Litt, B., Esteller, R., Echauz, J., D'Alessandro, M., Shor, R., Henry, T., Pennell, P., Epstein, C., Bakay, R. and Dichter, M. (2001) Epileptic Seizures May Begin Hours in Advance of Clinical Onset. A Report of Five Patients. *Neuron*, **30**(1), 51–64.

Molnar, P. and Nadler, J.V. (1999) Mossy Fiber-Granule Cell Synapses in the Normal and Epileptic Rat Dentate Gyrus Studied With Minimal Laser Photostimulation. *The Journal of Neurophysiology*, **82**(4), 1883–1894.

Mormann, F., Andrzejak, R.G., Kreuz, T., Rieke, Ch., David, P., Elger, Ch.E. and Lehnertz, K. (2003) Automated detection of a preseizure state based on a decrease in synchronization in intracranial electroencephalogram recordings from epilepsy patients. *Phys. Rev. E*, 67(2):021912, doi:10.1103/PhysRevE.67.021912.

Niedermeyer, E. and da Silva, F.L. (1999) *Electroencephalography, Basic Principles, Clinical Applications & Related Fields.* Williams and Wilkins, Baltimore (MD).

Pan, Y., Ge, S.S., Tang, F.R. and Mamun, A.A. (2007) Detection of epileptic spike-wave discharges using SVM. In: *Proceedings of the 2007 IEEE International Conference on Control Applications*, Suntec City, Singapore. IEEE, 467–472.

Pawlak, Z. (1991) Information Systems - Theoretical Foundations. *Information Systems Journal*, **6**, 205–218.

Racine, R.J. (1972) Modification of seizure activity by electrical stimulation: II. Motor seizure. *Electroencephalogr Clin Neurophysiol*, **32**, 281–294.

Raś, Z.W. and Dardzińska, A. (2005) Intelligent query answering. In: J. Wang, ed., *Encyclopedia of Data Warehousing and Mining*. Idea Group, 639–643.

Raś, Z.W., Tzacheva, A. and Tsay, L. (2005) Action Rules. In: J. Wang, ed., *Encyclopedia of Data Warehousing and Mining*. Idea Group, 1–5.

Raś, Z.W. and Wieczorkowska, A. (2000) Action Rules: how to increase profit of a company. *Principles of Data Mining and Knowledge Discovery*, **1910**, 87–592.

Salant, Y., Gath, I. and Henriksen, O. (1998) Prediction of epileptic seizures from two-channel EEG. *Medical and Biological Engineering and Computing*, **36**, 549–556.

Schiff, S.J., Jerger, K., Duong, D.H., Chang, T., Spano, M.L. and Ditto, W.L. (1994) Controlling chaos in the brain. *Nature*, **370**(6491), 615–620.

Stein, A.G., Eder, H.G., Blum, D.E., Drachev, A. and Fisher, R.S. (2000) An automated drug delivery system for focal epilepsy. *Epilepsy Res*, **39**(2), 103–114.

Tsay, L. and Raś, Z.W. (2005) Action Rules Discovery System DEAR Method and Experiments. *Journal of Experimental and Theoretical Artificial Intelligence*, **17**,1-2, 119–128.

Velasco, M., Velasco, F.V., Velasco, A.L., Boleaga, B., Jimenez, F., Brito, F. and Marquez, I. (2005) Double-blind randomized controlled pilot study of bilateral cerebellar stimulation for treatment of intractable motor seizures. *Epilepsia*, **46**(7), 1071–81.

White, A.M., Williams, P.A., Ferraro, D.J., Clark, S., Kadam, S.D., Dudek, F.E. and Staley, K.J. (2006) Efficient unsupervised algorithms for the detection of seizures in continuous EEG recordings from rats after brain injury. *Journal of Neuroscience Methods*, **152**(1-2), 255–266, ISSN 0165-0270, doi:DOI: 10.1016/j.jneumeth.2005.09.014.

Williams, P., White, A.M., Ferraro, D., Clark, S., Staley, K. and Dudek, F.E. (2006) The use of radiotelemetry to evaluate electrographic seizures in rats with kainate-induced epilepsy. *Journal of Neuroscience Methods*, **155**(1), 39–48, ISSN 0165-0270, doi:DOI: 10.1016/j.jneumeth.2005.12.035.

Williams, P.A., Hellier, J., White, A.M., Clark, S., Ferraro, D., Swiercz, W., Dudek, E.F. and Staley, K.J. (2009) Development of Spontaneous Recurrent Seizures after Kainate-Induced Status Epilepticus. *The Journal of Neuroscience*, **29**(7), 2103-–2112.

Williams, P.A., Hellier, J., White, A.M., Staley, K. and Dudek, E.F. (2007) Development of Spontaneous Seizures after Experimental Status Epilepticus: Implications for Understanding Epileptogenesis. *Epilepsia (Series 4)*, **48**, 157–163.

Williams, R.W. and Herrup, K. (1988) The Control of Neuron Number. *The Annual Review of Neuroscience*, **11**, 423–453.